Overdoped regime of the high-T_c superconductor $HgBa_2CuO_{4+\delta}$ and the relation between normal and superconducting carrier densities

R. Puźniak, R. Usami, and H. Yamauchi*

Superconductivity Research Laboratory, International Superconductivity Technology Center, 10-13 Shinonome 1-chome, Koto-ku, Tokyo 135, Japan

(Received 24 May 1995)

We have determined the ab-plane and c-axis components of penetration depth, λ_{ab} and λ_c, and coherence length, ξ_{ab} and ξ_c, for optimally doped (T_c=96 K) and overdoped $HgBa_2CuO_{4+\delta}$ (T_c=52 K). ξ_{ab}, ξ_c, and λ_{ab} increase, whereas λ_c decreases for the overdoped material in comparison to the optimally doped materials. Analysis of the data reveals that the increase of λ_{ab} is caused by a suppression of the superconducting carrier density n_s, and not an enhancement of the in-plane effective mass. The decrease of λ_c originates from an overcompensation in the suppression of n_s by a strongly reduced effective mass along the c axis.

In the phase diagram of high-T_c superconductors concerning the transition temperature T_c vs carrier concentration in the normal state n_n, three different regimes are usually distinguishable; (1) the underdoped region, where T_c increases with increasing doped hole concentration, (2) the optimally doped region, where T_c acquires a maximum value, and (3) the overdoped region, where T_c decreases with further doping.[1] Earlier investigations[2,3] of the influence of carrier density on the basic superconducting properties have been confined mostly to the underdoped and optimally doped regions. Studies of $La_{2-x}Sr_xCuO_4$ (La-214), $YBa_2Cu_3O_y$ (Y-123), and some other cuprate systems[2–5] found a remarkable correlation between T_c and the penetration depth, $\lambda^{-2}(T=0) \propto n_s/m^*$ (superconducting carrier density/effective mass). The superconducting transition temperature increases with increasing hole doping, with T_c being linearly proportional to λ^{-2}, and then shows saturation around the ''optimum'' doping level, where T_c is maximum.[6–8] Uemura *et al.*[9] reported that the muon spin relaxation rate $\sigma(T\rightarrow 0)$ ($\propto \lambda^{-2} \propto n_s/m^*$) in the overdoped region of $Tl_2Ba_2CuO_{6-\delta}$ (Tl-2201) decreases with increasing hole doping, implying that either n_s no longer scales with the normal-state carrier density n_n, and/or m_s^* for a superconducting pair becomes much larger than the value expected from the normal-state effective mass m_n^*. A similar relation between T_c and the depolarization rate $\sigma(T=0)$ was reported independently by Niedermayer *et al.*[10] Tallon *et al.*[11] showed that the depolarization rate ($\propto n_s/m^*$) of a variety of polycrystalline $YBa_2Cu_3O_{7-\delta}$, $Y_2Ba_4Cu_7O_{15-\delta}$, and $YBa_2Cu_4O_8$ samples increases when the crystals are fully oxygenated ($\delta\rightarrow 0$). These experimental results suggest that the behavior of high-T_c superconductors in the overdoped region is in marked contrast to that of conventional metallic superconductors, in which the normal-state properties (n_n, m_n^*, l), where l is the mean free path, directly represent the corresponding values in the superconducting state.

It is important to point out that one can only determine the ratio of superconducting carrier density to effective mass from muon spin-relaxation measurements.[3,12] Thus, it is not possible to distinguish between a decrease in the superconducting carrier density n_s with increasing hole carrier doping or a large increase in the effective mass of the superconducting pairs in the overdoped region. The first case may be described within a model of coexisting paired and unpaired fermions at $T\rightarrow 0$, whereas the second one may be due to the localization of superconducting pairs within the overdoped region.

In this paper we report an independent determination of n_s and m_s^* in the optimally doped and overdoped region of $HgBa_2CuO_{4+\delta}$ (Hg-1201). From measurements of the reversible magnetization we determined the thermodynamic parameters describing the superconducting state and have found a decrease in n_s, a saturation of the in-plane effective mass, and a decrease of the c-axis effective mass with increasing hole doping.

The nearly-single-phase[13] ceramic Hg-1201 (Ref. 14) was synthesized from a mixture of HgO, BaO, and CuO starting materials in an evacuated quartz tube at 650 °C for 1 h. The quality of the material was examined by powder x-ray diffraction with Cu$K\alpha$ radiation.[13] In the diffraction pattern no peaks of other phases were observed (see the x-ray-diffraction pattern of Hg-1201 in Ref. 15). The average diameter of crystalline grains, d, was (2.7±1.1) μm. In order to prepare samples with different carrier concentration, two types of annealing processes were performed: (i) annealing in flowing argon at 300 °C for 6 h and (ii) annealing in flowing oxygen at 200 °C for 6 h. The oxygen-annealed sample (T_c=52 K) was overdoped, whereas the argon-annealed sample (T_c=96 K) was slightly underdoped, but very close to the optimally doped region. We note that the relatively low annealing temperatures exclude the possibility of Hg loss. Optimally doped Hg-1201 has a relatively small anisotropy $\gamma=\lambda_c/\lambda_{ab}$ of about 1.8.[15] Schilling *et al.* reported for Hg-1223 an anisotropy between 17 and 27.[16] Reversible magnetization measurements for magnetically aligned Hg-1223 indicate an anisotropy of about 8.[17] Puzniak *et al.* estimated the anisotropy of Hg-1223 to be equal to approximately 5.[15] Laborde *et al.* found the anisotropy to decrease with decreasing number of copper-oxide planes for Hg-based materials.[18] All details concerning the relation between oxygen content, lattice constants, and transition temperature in the optimally doped and overdoped regions of Hg-1201 were recently published by Tokiwa-Yamamoto *et al.*[19] Temperature dependences of the field-cooled dc magnetic susceptibil-

ity measured with a superconducting quantum interference device (SQUID) magnetometer in a magnetic field of 10 Oe indicated a sharp transition from the normal to superconducting states. The measured shielding signal was in the range 40–50 % of the completely diamagnetic response, in agreement with the expected value for the granular superconductor when $\lambda/d \geqslant 0.1$ (the λ value of the Hg-1201 is larger than 0.25 μm). The ratio of Meissner (field-cooled) to zero-field-cooled signals was above 90%, even at the lowest temperature of 5 K.

To perform measurements of anisotropic properties, oriented material is required. Therefore, we mechanically powdered the bulk samples, mixed the powder with a resin and applied a magnetic field of 8 T at room temperature for 24 h, in a similar manner to that developed by Farrell *et al.*[20] for the grain alignment of $YBa_2Cu_3O_{7-\delta}$. Finally, grain-aligned samples,[13,15] in which the average crystallographic c axis is parallel to the cylindrical axis of the solidified resin holder, were obtained. The x-ray data[13] indicate that for both samples the intensities of peaks other than **001** are negligibly small.

The superconducting-state thermodynamic parameters were derived from measurements of the reversible dc magnetization $M(H,T)$ in magnetic fields $H_{c1} \ll H \ll H_{c2}$, applied both parallel ($\mathbf{H} \| c$) and perpendicular ($\mathbf{H} \perp c$) to the c axis. Within such a range of field the reversible magnetization M is known to be linearly proportional to $\ln H$ such that[21,22]

$$M(H) = -[\Phi_0/32\pi^2\lambda_{ab}^2(T)]\ln(\eta H_{c2}/eH), \qquad (1)$$

for **H** parallel to the c axis. Here Φ_0 is the flux quantum, H_{c2} is the upper critical field in the direction of applied field, and η is a constant of the order of unity. The reversible magnetization for **H** perpendicular to the c axis is given by a modification of Eq. (1) with $\lambda_{ab}^2(T)$ replaced by $\lambda_{ab}(T)\lambda_c(T)$. Thermal fluctuation effects are negligible in materials with a small anisotropy,[22–24] and the simple London formulas shown above give a quantitatively correct description of the reversible magnetization of Hg-1201.

Magnetic measurements of grain-aligned Hg-1201 samples were performed using a commercial 5.5-T SQUID magnetometer (Quantum Design). The $M(H)$ data were collected in the "step-by-step mode" for increasing and decreasing magnetic fields ranging from 17.5 to 35 kOe. The measurements were performed at relatively low temperatures, at and above 40 K and 35 K for optimally doped and overdoped Hg-1201 samples, respectively. The lower temperature limits are imposed because of the appearance of irreversibility in the field dependent magnetization, the higher limits to avoid the influence of any thermal fluctuations.[22,23]

The experimental points M vs H are well described by a logarithmic dependence on applied field [Eq. (1)], $M(H) = -K_1 + K_2 \times \ln(H)$, where K_1 and K_2 are constants for a fixed temperature, oxygen concentration, and sample orientation with respect to the applied magnetic field. The imperfect orientation of the crystalline grains of magnetically aligned samples has an influence on measured M-vs-H dependences. Scanning-electron-microscopy measurements confirmed that the c axis of single grains was oriented along the applied magnetic field. However, in our powdered material, there were few grain conglomerates that were randomly oriented. We estimated the fraction of nonaligned grains in our samples to be 22 ± 8 %. The above estimates allow us to describe the reversible magnetization data, as a sum of two contributions: that of aligned grains resulting from Eq. (1), and that of the average magnetization of nonoriented grains.[21] Corrections due to the imperfect alignment of grains, on the determination of penetration depths, were performed as in Ref. 15. It is important to notice that the error caused by imperfect alignment is small if the anisotropy of the material is small.[15]

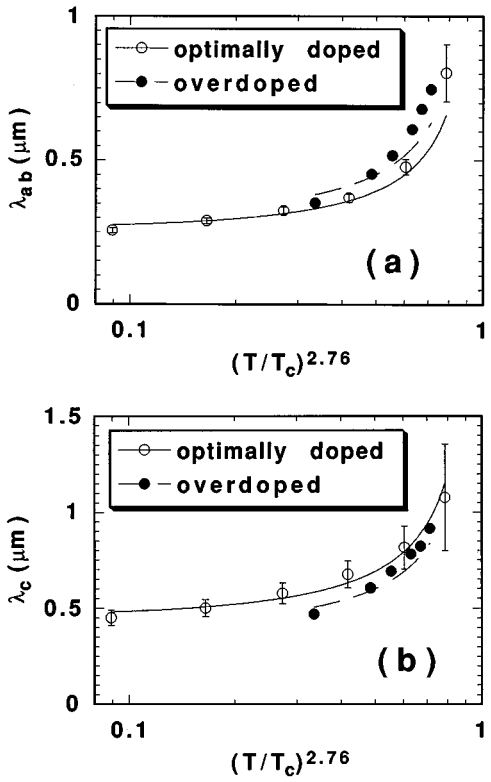

FIG. 1. Temperature dependence of the ab-plane (a) and the c-axis (b) components of the penetration depth for optimally doped and overdoped Hg-1201. The lines fitted to the experimental points are given by the formula $\lambda(T) = \lambda(0)/[1-(T/T_c)^{2.76}]^{0.6}$.

The penetration depths in the ab plane and along the c axis, λ_{ab} and λ_c, for the optimally doped and overdoped samples, as derived from the experimental data, are plotted in Figs. 1(a) and 1(b). The curves given in Fig. 1 are fitted to the experimental points applying an empirical rule; $\lambda(T) = \lambda(0)/[1-(T/T_c)^A]^B$, where $\lambda(0)$ is a fitting parameter, and A and B are constants equal to 2.76 and 0.6, respectively. This formula approximates well to the temperature dependence of the penetration depth, over a wide range of temperature in the clean BCS limit. The presented data clearly indicate that the ab-plane component of the penetration depth $\lambda_{ab}(T=0)$ increases in the overdoped region, whereas the c-axis component $\lambda_c(T=0)$ decreases. The extrapolated zero temperature values of the components of penetration depth are equal to 260 ± 6 nm and 298 ± 11 nm for λ_{ab} and 454 ± 10 nm and 395 ± 12 nm for λ_c in optimally doped and overdoped regions, respectively.

The upper critical fields parallel to the c axis, $H_{c2\|c}$, for optimally doped and overdoped samples, obtained using Eq. (1) with η being set at 1.4 (Ref. 22) are plotted in Fig. 2. The

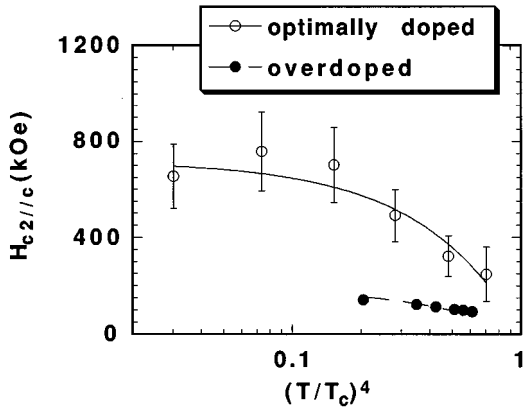

FIG. 2. Temperature dependence of the upper critical field parallel to the c axis. The lines fitted to the experimental points are given by formula $H_{c2\|c}(T)=H_{c2\|c}(0)\times[1-(T/T_c)^4]$.

lines fitted to the experimental points are given by the formula $H_{c2}(T)=H_{c2}(0)\times[1-(T/T_c)^4]$. There is a far larger uncertainty in the determination of H_{c2} than of λ. This is because of an insufficient knowledge of the structural parameter η of the flux lattice as well as its angular dependence.[21] Nevertheless, a decrease of H_{c2} in the overdoped region of Hg-1201 is evident. Extrapolated to zero temperature, the values of upper critical field for the $\mathbf{H}\|c$ axis are equal to 72 T in the optimally doped and 19.4 T in the overdoped region. Related values of the ab-plane components of coherence length, $\xi_{ab}=(\Phi_0/2\pi H_{c2\|c})^{1/2}$, are equal to 21.1 Å for the optimally doped and 41.1 Å for the overdoped region. $H_{c2\perp c}$ and ξ_c were determined applying the relations $H_{c2\perp c}=\gamma H_{c2\|c}$ and $\xi_c=\xi_{ab}/\gamma$ for the previously estimated values of $H_{c2\|c}$ and ξ_{ab}. Values of 125 and 25.7 T for $H_{c2\perp c}(0)$ and 12.1 and 31 Å for $\xi_c(0)$ were obtained for optimally doped and overdoped samples, respectively.

The thermodynamic superconducting state parameters are tabulated in Table I. The values of the lower critical field, $H_{c1\|c}$, were calculated using the formula[25]

$$H_{c1\|c}=\Phi_0/4\pi\lambda_{ab}{}^2[\ln(\lambda_{ab}/\xi_{ab})+0.5], \tag{2}$$

TABLE I. Anisotropic superconducting-state thermodynamic parameters for optimally doped and overdoped Hg-1201.

Quantity/Phase	Optimally doped	Overdoped
T_c (K)	96	52
n_s (cm^{-3})	7.8×10^{20}	5.5×10^{20}
m^*_{ab}/m_e	1.9	1.7
m^*_c/m_e	5.7	3.0
$\lambda_{ab}(0)$ (nm)	260	298
$\lambda_c(0)$ (nm)	454	395
$\gamma=\lambda_c(0)/\lambda_{ab}(0)$	1.8	1.3
$\xi_{ab}(0)$ (Å)	21.1	41.1
$\xi_c(0)$ (Å)	12.1	31.0
$H_{c1\|c}(0)$ (Oe)	129	89
$H_{c1\perp c}(0)$ (Oe)	82	71
$H_{c2\|c}(0)$ (T)	72	19.4
$H_{c2\perp c}(0)$ (T)	125	25.7

with the values of λ_{ab} and ξ_{ab} as given in Table I. The values of $H_{c1\perp c}$ were calculated using a modification of Eq. (2) with $\lambda_{ab}{}^2$ replaced by $\lambda_{ab}\lambda_c$ and (λ_{ab}/ξ_{ab}) replaced by $(\lambda_{ab}\lambda_c/\xi_{ab}\xi_c)^{1/2}$.

The experimentally determined λ and ξ are related to n_s, m^*, and ξ/l. Since for most of the cuprate superconductors the ab-plane mean free path is much higher than the coherence length ξ_{ab},[26] the in-plane properties can be described within the clean-limit approximation. In material with a small anisotropy, a similar relation between l and ξ should also be true along the c axis. Therefore, the relation between penetration depth, superconducting carrier concentration, and effective mass for Hg-1201 can be given within the clean-limit approximation by the formula[27]

$$\lambda^{-2}=4\pi n_s e^2/(m^*_s c^2), \tag{3}$$

with m^*_s substituted by m^*_{ab} and m^*_c for the ab-plane and the c-axis components of the penetration depth, respectively.

Equation (3) relates two experimentally measurable variables, λ_{ab} and λ_c, to the superconducting carrier density n_s and carrier effective masses, m^*_{ab} and m^*_c. To determine the values of the above parameters, i.e., values of n_s, m^*_{ab}, and m^*_c, it is necessary to derive at least one more equation relating measurable variables, for example, coherence length with carrier concentration and effective mass. For a free electron gas in three dimensions the Fermi temperature can be related to the Sommerfeld constant γ and to the muon spin-relaxation rate σ by[3,28,29]

$$k_B T_F=E_F=\hbar^2/2m^*_{a\nu}(3\pi^2 n)^{2/3}\propto\sigma^{3/4}\gamma^{-1/4}. \tag{4}$$

Since the Hg-1201 superconductor is characterized by rather small anisotropy, the approximation of the Fermi temperature by Eq. (4) does not seem to be wholly unreasonable. For materials with effective mass fully characterized by two components, $m^*_{ab}=m^*_a=m^*_b$ and m^*_c, the average effective mass $m^*_{a\nu}$ is equal to $(m^{*2}_{ab}m^*_c)^{1/3}$. The relation between the ab-plane and the c-axis components of the wave vector at the Fermi surface, k_{Fab} and k_{Fc}, is given by $(\hbar k_{Fab})^2/2m^*_{ab}=(\hbar k_{Fc})^2/2m^*_c$. Then, the velocity at the Fermi surface ν_F in the ab plane is given by:

$$\nu_{Fab}=\hbar k_{Fab}/m^*_{ab}=\hbar/(m^{*5}_{ab}m^*_c)^{1/6}(3\pi^2 n)^{1/3} \tag{5}$$

and along the c axis by

$$\nu_{Fc}=\hbar k_{Fc}/m^*_c=\hbar/(m^*_{ab}m^{*2}_c)^{1/3}(3\pi^2 n)^{1/3}. \tag{6}$$

The coherence length is proportional to the velocity at the Fermi level and inversely proportional to T_c, according to the relation[30]

$$\xi=a(\hbar\nu_F/k_B T_c). \tag{7}$$

The parameter a determined empirically by Pippard is equal to 0.15.[30] The microscopic BCS theory gives Eq. (7) with $a=0.18$. The values of n_s, m^*_{ab} and m^*_c determined from λ_{ab}, λ_c, ξ_{ab}, and ξ_c, using Eqs. (3) and (5)–(7) with $a=0.18$, are presented in Table I. The results indicate a decrease in the superconducting carrier density from 7.8×10^{20} cm^{-3} in optimally doped material ($T_c=96$ K) to 5.5×10^{20} cm^{-3} in the overdoped region of Hg-1201 ($T_c=52$ K). Such a change corresponds to a decrease in the superconducting

carrier density from 0.11 carriers per formula unit in optimally doped material to 0.078 carriers per formula unit in overdoped Hg-1201. Importantly, we find a lower $n_s(T\rightarrow 0)$ in a material characterized by a higher carrier density in the normal state. The ab-plane components of superconducting carrier effective mass do not increase in the overdoped region of Hg-1201. A decrease of the c-axis component of the effective mass from $m^*/m_e=5.7$ in the optimally doped region to 3.0 in the overdoped region is clearly evident. Therefore, a localization of the superconducting pairs in the overdoped region can be excluded. The obtained results may indicate that in the superconducting materials not all the carriers become superconducting at low temperature. That is, there is a coexistence of paired and unpaired fermions in the overdoped region of high-T_c superconductors at $T\rightarrow 0$.

Concluding, we have determined the superconducting carrier density and effective mass in the optimally doped and overdoped region of Hg-1201 and have found a decrease of the superconducting carrier density with increasing hole doping. We did not observe an increase of effective mass with increasing hole doping and therefore, exclude localization of the superconducting pairs in the overdoped region of Hg-1201.

We thank Dr. J. Schützmann for useful discussions and for critical reading of the manuscript. This work was supported by NEDO for the R&D of Industrial Science and Technology Frontier Program.

*Present address: Tokyo Institute of Technology, Research Laboratory of Engineering Materials, Nagatsuta, Midori-ku, Yokohama 226, Japan.

[1] Y. Kubo, Y. Shimakawa, T. Manako, and H. Igarashi, Phys. Rev. B **43**, 7875 (1991).
[2] Y. J. Uemura *et al.*, Phys. Rev. Lett. **62**, 2317 (1989).
[3] Y. J. Uemura *et al.*, Phys. Rev. Lett. **66**, 2665 (1991).
[4] B. Pümpin *et al.*, Phys. Rev. B **42**, 8019 (1990).
[5] C. L. Seaman *et al.*, Phys. Rev. B **42**, 6801 (1990).
[6] T. Schneider and H. Keller, Phys. Rev. Lett. **69**, 3374 (1992).
[7] H. Zhang and H. Sato, Phys. Rev. Lett. **70**, 1697 (1993).
[8] Y. J. Uemura, G. M. Luke, and L. P. Le, Synth. Met. **56**, 2845 (1993).
[9] Y. J. Uemura *et al.*, Nature (London) **364**, 605 (1993).
[10] Ch. Niedermayer *et al.*, Phys. Rev. Lett. **71**, 1764 (1993).
[11] J. L. Tallon *et al.*, Phys. Rev. Lett. **74**, 1008 (1995).
[12] W. Barford and J. M. F. Gunn, Physica C **156**, 515 (1988).
[13] R. Usami *et al.*, in *Advances in Superconductivity VI*, edited by T. Fujita and Y. Shiohara (Springer, Tokyo, 1994), p. 331.
[14] S. N. Putilin, E. V. Antipov, O. Chimaissem, and M. Marezio, Nature (London) **362**, 226 (1993).
[15] R. Puzniak, R. Usami, K. Isawa, and H. Yamauchi, Phys. Rev. B **52**, 3756 (1995).
[16] A. Schilling *et al.*, Physica C **235-240**, 229 (1994).
[17] Y. C. Kim *et al.*, Phys. Rev. B **51**, 11 767 (1995).
[18] O. Laborde, B. Souletie, J. L. Tholence, and J. J. Capponi, Solid State Commun. **90**, 443 (1994).
[19] A. Tokiwa-Yamamoto *et al.*, ISTEC J. **7**(2), 11 (1994).
[20] D. E. Farrell *et al.*, Phys. Rev. B **36**, 4025 (1987).
[21] V. G. Kogan, M. M. Fang, and S. Mitra, Phys. Rev. B **38**, 11 958 (1988).
[22] V. G. Kogan *et al.*, Phys. Rev. Lett. **70**, 1870 (1993).
[23] L. N. Bulaevskii, M. Ledvij, and V. G. Kogan, Phys. Rev. Lett. **68**, 3773 (1992).
[24] A. Schilling, R. Jin, J. D. Guo, and H. R. Ott, Physica B **194-196**, 2185 (1994).
[25] G. Burns, *High-Temperature Superconductivity* (Academic, Boston, 1992).
[26] K. Kamaras *et al.*, Phys. Rev. Lett. **64**, 84 (1990).
[27] P. G. de Gennes, *Superconductivity of Metals and Alloys* (Benjamin, New York, 1966).
[28] Y. J. Uemura, Physica C **185-189**, 733 (1991).
[29] D. R. Harshman, and A. P. Mills, Jr., Phys. Rev. B **45**, 10 684 (1992).
[30] B. S. Chandrasekhar, in *Superconductivity*, edited by R. D. Parks (Marcel Dekker, New York, 1969), p. 1.